

UC Berkeley

UC Berkeley Previously Published Works

Title

Molecular weaving of chicken-wire covalent organic frameworks

Permalink

<https://escholarship.org/uc/item/9vv8d9dq>

Journal

Chem, 9(9)

ISSN

1925-6981

Authors

Han, Xing

Ma, Tianqiong

Nannenga, Brent L

et al.

Publication Date

2023-09-01

DOI

10.1016/j.chempr.2023.07.015

Copyright Information

This work is made available under the terms of a Creative Commons Attribution License, available at <https://creativecommons.org/licenses/by/4.0/>

Peer reviewed

Molecular Weaving of Chicken Wire Covalent Organic Frameworks

Xing Han^{1,2}, Tianqiong Ma^{1,2}, Brent L. Nannenga^{3,4}, Xuan Yao⁵, S. Ephraim Neumann^{1,2}, Punit Kumar^{6,7}, Junpyo Kwon^{6,7}, Zichao Rong^{1,2}, Kaiyu Wang^{1,2}, Yuebiao Zhang⁵, Jorge A. R. Navarro⁸, Robert O. Ritchie^{6,7}, Yong Cui^{9,*}, and Omar M. Yaghi^{1,2,*}

¹Department of Chemistry and Kavli Energy Nanoscience Institute, University of California, Berkeley, 94720, CA, United States.

²Bakar Institute of Digital Materials for the Planet, Division of Computing, Data Science, and Society, University of California, Berkeley, 94720, CA, United States.

³Chemical Engineering, School for Engineering of Matter, Transport and Energy, Arizona State University, Tempe, AZ 85287, United States.

⁴Center for Applied Structural Discovery, The Biodesign Institute, Arizona State University, Tempe, AZ, United States.

⁵Shanghai Key Laboratory of High-Resolution Electron Microscopy, School of Physical Science and Technology, ShanghaiTech University, Shanghai, 201210, China.

⁶Materials Science Division, Lawrence Berkeley National Laboratory, Berkeley, CA, 94720, United States.

⁷Department of Mechanical Engineering, Department of Materials Science & Engineering, University of California, Berkeley, CA, 94720, United States.

⁸Department of Inorganic Chemistry, Universidad de Granada, 18071 Granada, Spain.

⁹School of Chemistry and Chemical Engineering, Frontiers Science Center for Transformative Molecules and State Key Laboratory of Metal Matrix Composites, Shanghai Jiao Tong University, Shanghai, 200240, China.

*Corresponding authors. Email: yongcui@sjtu.edu.cn, yaghi@berkeley.edu.

Abstract: Molecular weaving is the interlacing of covalently linked threads to make extended structures. Although weaving based on three-dimensional networks has been reported, the two-dimensional forms remain largely unexplored. Reticular chemistry uses mutually embracing tetrahedral metal complexes as crossing points, which when linked typically lead to 3D woven structures. Realizing two-dimensional weaving patterns requires crossing points with an overall planar geometry. We show that polynuclear helicates composed of multiple metal-complex units, and therefore multiple turns, are well-suited in this regard. By reticulating helicate units, we successfully obtained two-dimensional weaving structures based on the familiar chicken wire pattern.

The power of reticular chemistry has been illustrated in making metal-organic frameworks (MOFs) and covalent organic frameworks (COFs) with predetermined structures¹. Recently, molecular weaving has further expanded this chemistry by using either weak intermolecular forces or mutually embracing metal complexes to create woven structures wherein long threads are interlaced²⁻⁸. Previous work has employed such complexes with an overall tetrahedral geometry to consistently give 3D woven and interlocked frameworks⁵⁻⁸. In our attempt to expand the scope of this chemistry, we asked the question of how one maintains the necessity of having mutually embracing complexes for weaving to take place, while at the same time, targeting topologies other than 3D networks. Namely, how do we prepare woven 2D structures? We believe that such arrangements are of fundamental importance to achieving properties, which make woven fabric and metal fences so pervasive in our society. In this work, we show how helicates⁹⁻¹² composed of multiple mutually embracing complexes can indeed be used to access the very planar building units necessary for making 2D patterns. By controlling the number of turns in these helical building units, we show that two distinct chicken wire patterns are achieved (Fig. 1).

The key to designing new molecular weaving patterns is to choose a mutually embracing metal complex, which serves as a crossing point. The linking groups (points-of-extension) define its overall geometry, and in reticulating an extended woven structure there are three factors to be considered: 1) The angles between these geometric units determine the dimensionality of the woven pattern, 2) the directionality of the points-of-extension control the propagation of the structure, and 3) the relative orientation of the units bearing the points-of-extension will ultimately determine the type of pattern. The latter factor is especially useful when using helicates because of their chirality: an aspect typically not considered in MOF or COF construction, but essential to molecular weaving by design (Fig. 1a, b). In our pursuit of 2D weaving, we use two- and three-turn helicates to illustrate how two patterns can be achieved, where the threads either propagate orthogonally or parallel to each other (Figs. 1c, d).

Our synthetic strategy is shown in Fig. 2. The weaving nodes dicopper(I)-bis{4,4'-[1,3-phenylenebis(1,10-phenanthroline-9,2-diyl)] dibenzaldehyde}tetrafluoroborate, $\text{Cu}_2(\text{PPD})_2(\text{BF}_4)_2$, and

Tricopper-bis{2,9-bis[3-(9-(4-(dimethoxymethyl)phenyl)-1,10-phenanthrolin-2-yl)phenyl]-1,10-phenanthroline}tritetrafluoro-borate, $\text{Cu}_3(\text{DPPP})_2(\text{BF}_4)_3$, can be functionalized with either aldehyde or dimethoxymethyl groups. The functional groups can be linked with 9,10-bis(4-aminophenyl)anthracene (BAA) or 2,7-bis(4-aminophenyl)pyrene (BAP), respectively, to make imine-bonded PPD-BAA or DPPP-BAP threads. These two complexes include two and three copper(I) ions, respectively, and have been studied extensively as discrete molecules for the formation of molecular knots^{13,14}. The single-crystal structures of the complexes and their analogues confirm a pseudo planar geometry at the helicate edges, which ensures the assembly of the threads into a 2D framework (Figs. 1a, b, Supplementary Figs. 1, 2), resembling a chicken wire. Mechanical measurements by AFM nanoindentation indicate that the 2D structures have a higher elasticity compared to the reported 3D woven structures. Upon removal of the Cu(I) ions, the threads become solely held together by mechanical bonds, thereby making the material even more elastic.

Results and discussion

Synthesis and characterization. The synthesis of COF-524-Cu, $[\text{Cu}_2(\text{PPD})_2(\text{BF}_4)_2(\text{PPA})_2]_{\text{imine}}$ or COF-525-Cu, $[\text{Cu}_3(\text{DPPP})_2(\text{BF}_4)_3(\text{BAP})_2]_{\text{imine}}$ was carried out using equimolar amounts of $\text{Cu}_2(\text{PPD})_2(\text{BF}_4)_2$ or $\text{Cu}_3(\text{DPPP})_2(\text{BF}_4)_3$ and BAA or BAP, which were reacted in dioxane or a 1:3 (v/v) mixture of *N,N*-Dimethylacetamide (DMA) and chlorobenzene in the presence of aqueous acetic acid as a catalyst. The reaction mixture was sealed in a Pyrex tube and heated at 120 °C. After 7 days, the resulting precipitate was collected and washed by Soxhlet extraction with anhydrous tetrahydrofuran to yield a dark brown crystalline solid, which was found to be insoluble in common organic solvents and water. The formation of imine linkages in the COFs was confirmed by Fourier-transform infrared (FT-IR) spectroscopy (Supplementary Figs. 3, 4). and ¹³C cross-polarization magic angle spinning (CP-MAS) solid-state NMR spectroscopy (Supplementary Figs. 5, 6). The FT-IR spectra of COF-524-Cu and COF-525-Cu feature characteristic C=N stretching vibrations at 1665 and 1656 cm^{-1} , respectively,

corroborating the formation of imine bonds. The formation of imine linkages was further confirmed by ^{13}C CP-MAS NMR solid-state NMR spectroscopy, with the characteristic C=N imine resonance being observed at 158 ppm, which can be differentiated from the C=N double bond of the phenanthroline unit located at around 152 ppm. Additionally, the disappearance of resonances above 192 ppm for COF-524-Cu, as well as 54 ppm and 100 ppm for COF-525-Cu demonstrate full conversion of the $\text{Cu}_2(\text{PPD})_2(\text{BF}_4)_2$ aldehyde and $\text{Cu}_3(\text{DPPP})_2(\text{BF}_4)_3$ dimethyl acetal starting material. These results support completeness of the reaction and formation of imine bonds between the building blocks to form an extended framework structure. Their thermal stability of both COFs studied by TGA measured under a N_2 atmosphere, and the onset of the thermal decomposition of both COFs were found to be at $\sim 400^\circ\text{C}$ (Supplementary Fig 7). Both COFs exhibited powder X-ray diffraction (PXRD) patterns with sharp peaks and low background that match the predicted patterns of the simulated structures (Fig. 3).

Structure determination. Scanning electron microscopy (SEM) micrographs show a homogeneous morphology of rod-shaped crystals for COF-524-Cu (Supplementary Fig. 8) and prism-shaped crystals for COF-525-Cu. (Fig. 4a). After ultrasonication of the sample in isopropanol, individual COF crystals were dispersed on a copper sample grid for transmission electron microscopy (TEM) analysis. 3D electron diffraction tomography (3D-EDT) data of COF-524-Cu was collected by combining specimen tilt and electron-beam tilt in the range of -49.6° to $+50.6^\circ$ with a beam-tilt step of 0.3° and was further processed by an EDT-process program^{15,16}. From the acquired data set the 3D reciprocal lattice of COF-524-Cu was constructed and found to have unit-cell parameters of $a = 25.01 \text{ \AA}$, $b = 19.99 \text{ \AA}$, $c = 12.20 \text{ \AA}$, and $V = 6099.4 \text{ \AA}^3$, $\alpha = \beta = \gamma = 90^\circ$. From the acquired data, a structural model of COF-524-Cu was built in Materials Studio 8.0 in the orthorhombic space group $P222$. The unit-cell parameters were optimized further by Pawley refinement of the PXRD pattern to be $a = 25.84 \text{ \AA}$, $b = 20.76 \text{ \AA}$, $c = 12.87 \text{ \AA}$, and $V = 6904.0 \text{ \AA}^3$ ($R_{wp} = 1.30\%$, $R_p = 0.97\%$). The calculated PXRD pattern of the modeled structure was found to be in good agreement with the experimental pattern of COF-524-Cu (Fig. 3a, Supplementary Section 8.1).

For COF-525-Cu, a single crystal was identified and analyzed using microcrystal electron diffraction (MicroED)^{17,18}. The microED data set was collected by rotating the crystal by 65° in the electron beam at a rate of 1.0° per second. The diffraction data set was processed to 1.71 Å using XDS¹⁹ to identify the unit cell parameters and space group, which were determined to be *C*222, $a = 18.45$ Å, $b = 30.68$ Å, $c = 15.61$ Å, and $V = 8836$ Å³ (Figs. 3b, 4b, Supplementary Sections 8.2). The structural model of COF-525-Cu was constructed based on this information, and the simulated PXRD pattern showed great alignment with the experimental pattern. The unit-cell parameters were further optimized by Pawley refinement of the PXRD pattern to be $a = 18.45$ Å, $b = 31.08$ Å, $c = 16.00$ Å, and $V = 9181$ Å³ with very low discrepancy factors ($R_p = 1.02\%$, $R_{wp} = 1.56\%$; Fig. 3b).

According to the refined model, COF-525-Cu crystallizes in hexagonal wire meshes by pseudo-square-planar building units $\text{Cu}_3(\text{DPPP})_2(\text{BF}_4)_3$ and linear linkers BAP connected through imine bonds. Covalently linked 1D zigzag threads propagate along the crystallographic *c*-axis and adjacent parallel threads are mechanically braided by triple-turn helicates at each crossing point, thus forming a chicken wire motif with 32.0×62.2 Å meshes along the crystallographic *b*-axis (Fig. 5b). These 2D frameworks are two-fold interpenetrated along the *b*-axis with each layer staggered along the *a*-axis (AB-stacking) and leave enough space for the BF_4^- counterions (Fig. 5d). High-resolution TEM (HRTEM) images were collected to gain further insight into the crystal structure of COF-525-Cu. The striped pattern of the lattice fringes observed in the HRTEM image shown in Fig. 4d, which are separated by 16.1 Å and 15.2 Å, are in good agreement with the copper ions located within each crossing point.

We note that in the context of reticular chemistry, the number of turns in the crossing points directs how the threads are woven in the crystalline network. By substituting the triple-turn helicates with double-turn helicates, we were able to synthesize COF-524-Cu, which also exhibits the expected pattern of two-fold interpenetrated chicken wire weaving with staggered stacking (Figs. 5a, c). The average background subtraction filter (ABSF) HRTEM image of COF-524-Cu was taken along the [010] direction. The striped pattern of the lattice fringes observed in the HRTEM image shown in Supplementary Fig. 11, which are

separated by 12.87 Å and 12.92 Å, are in good agreement with the structural model viewed along the [010] direction. However, unlike the motif observed in COF-525-Cu, in which the structural pattern is formed by the weaving of zigzag threads with two adjacent parallel threads, in COF-524-Cu, the two sets of diagonal linear threads propagate in an opposite direction. The diagonal blue and yellow linear threads are woven to form the 2D structure with 25.7×51.7 Å meshes and each of the threads is periodically crossing all threads that are orthogonal to it (Fig. 5a). Although COF-524-Cu and -525-Cu are all composed of homochiral helicates in one crystal domain, the mixed enantiomeric isomers give rise to overall racemic woven frameworks.

We sought to remove the Cu ions and examine the properties of the materials before and after demetalation. Heating the COFs in a KCN solution of *n*-butanol/water (3:1) yielded metal-free structures. Using inductively coupled plasma atomic emission spectroscopy (ICP-AES), we confirmed that 94 to 97% of the Cu(I) copper ions had been removed (Supplementary Table 5). The dark brown or red color of COF-524-Cu and -525-Cu changed to pale yellow or gray for COF-524 and -525 as the demetalation proceeded (Supplementary Figs 12, 13). As expected, the crystallinity of the demetalated material decreased compared to the pristine COFs (Supplementary Figs 14, 15). The SEM images show similar morphology and crystal sizes before and after demetalation (Supplementary Figs 8, 18). Additionally, the imine linkages were also maintained throughout the process: The characteristic FT-IR stretches at 1665 and 1656 cm^{-1} are consistent with those of COF-524 and -525, respectively (Supplementary Figs 16, 17). Furthermore, the material could be remetalated with Cu(I) ions by stirring in a $\text{CH}_3\text{CN}/\text{CH}_2\text{Cl}_2$ solution of $\text{Cu}(\text{CH}_3\text{CN})_4\text{BF}_4$ to give back crystalline COF-524-Cu and -525-Cu. These remetalated COFs have similar crystallinity to the original as-synthesized COFs, as evidenced by the retention of the intensity and positions of the peaks in the PXRD patterns (Supplementary Figs 14, 15). In the FT-IR spectrum, the peak representing the imine C=N stretch was retained, indicating that the framework is chemically stable and robust under such reaction conditions (Supplementary Figs 16, 17).

We measured the mechanical properties of a single particle of the metalated and demetalated COFs using nano-indentation. The Young's moduli of COF-524-Cu and -525-Cu were 3.41 (± 0.72) and 2.38 (± 0.74) GPa, respectively, which is significantly more elastic than the reported values for the 3D woven COF-505⁸ and wCOF-Ag²⁰ and a similar order of magnitude to other reported values of 2D COFs²¹ or common polymers^{22,23}. The hardness values of COF-524-Cu and -525-Cu were 124.79 (± 46.61) and 92.82 (± 33.50) MPa, respectively. The results indicate that COF-525-Cu is mechanically more flexible and softer than COF-524-Cu; highlighting the importance of designing parallel alignment patterns of woven threads to control the material's properties (Supplementary Figs. 19-21). The COF-525-Cu's parallel alignment of its woven helicate threads is structurally advantageous for their mechanical folding along the crystallographic *b*-axis. By contrast, the crosslinked alignment of the woven helicate threads of COF-524-Cu prevents the folding. Moreover, the demetalation process can further enhance their mechanical flexibility (2.28 (± 0.75) and 1.56 (± 0.64) GPa for COF-524 or -525, respectively), which is attributed to the increased degree of freedom due to the loose interactions between the threads upon the removal of copper ions.

Conclusion

We developed a new approach to achieve 2D woven COFs by installing functionalized polynuclear helicates. The pseudo-planar square geometry of the helicate linkers not only allows us to access 2D frameworks, closely resembling chicken wire fences, but also offers precise control over the type of pattern. The helical even and odd turn numbers directly influence the resulting woven pattern and its mechanical properties. This strategy enables the generation of a new class of woven COFs.

Methods

Synthesis of COF-524-Cu: A Pyrex tube measuring 10 × 8 mm (o.d × i.d) was charged with $\text{Cu}_2(\text{PPD})_2(\text{BF}_4)_2$ (8 mg, 0.005 mmol), BAA (3.6 mg, 0.01 mmol), 1 mL of anhydrous dioxane and 0.4 mL of 6 M aqueous acetic acid solution. The tube was flash frozen at 77 K (liquid N_2 bath), evacuated to an internal pressure of 50 mTorr and flame sealed. Upon sealing, the length of the tube was reduced to 13-15 cm. The reaction was heated at 120 °C for 7 days yielding a brown solid at the bottom of the tube which was isolated by centrifugation and washed with anhydrous THF and dried at 120 °C under 50 mTorr for 12 h. This material is insoluble in water and common organic solvents such as hexanes, methanol, acetone, tetrahydrofuran, *N,N*-dimethylformamide, and dimethyl sulfoxide, indicating the formation of an extended structure. Yield: 9.7 mg, 86.3% based on $\text{Cu}_2(\text{PPD})_2(\text{BF}_4)_2$.

Synthesis of COF-525-Cu: A Pyrex tube measuring 10 × 8 mm (o.d × i.d) was charged with $\text{Cu}_3(\text{DPPP})_2(\text{BF}_4)_3$ (12.2 mg, 0.005 mmol), BAP (3.8 mg, 0.01 mmol), 0.3 mL of *N,N*-dimethylacetamide (DMA), 0.7 mL of chlorobenzene (CB), and 0.1 mL of 6 M aqueous acetic acid solution. The tube was flash frozen at 77 K (liquid N_2 bath), evacuated to an internal pressure of 50 mTorr and flame sealed. Upon sealing, the length of the tube was reduced to 13-15 cm. The reaction was heated at 120 °C for 3 days yielding a brown solid at the bottom of the tube which was isolated by centrifugation and washed with anhydrous THF and dried at 120 °C under 50 mTorr for 12 h. This material is insoluble in water and common organic solvents such as hexanes, methanol, acetone, tetrahydrofuran, *N,N*-dimethylformamide, and dimethyl sulfoxide, indicating the formation of an extended structure. Yield: 9.7 mg, 86.3% based on $\text{Cu}_3(\text{DPPP})_2(\text{BF}_4)_3$.

References

1. Yaghi, O. M., Kalmutzki, M. J. & Diercks, C. S. Introduction to Reticular Chemistry: Metal–Organic Frameworks and Covalent Organic Frameworks (Wiley-VCH, 2019).
2. Lewandowska, U.; Zajaczkowski, W.; Corra, S.; Tanabe, J.; Borrmann, R.; Benetti, E. M.; Stappert, S.; Watanabe, K.; Ochs, N. A. K.; Schaeublin, R.; Li, C.; Yashima, E.; Pisula, W.; Müllen, K.; Wennemers, H., A triaxial supramolecular weave. *Nat. Chem.* **9**, 1068-1072 (2017).
3. August, D. P.; Dryfe, R. A. W.; Haigh, S. J.; Kent, P. R. C.; Leigh, D. A.; Lemonnier, J.-F.; Li, Z.; Muryn, C. A.; Palmer, L. I.; Song, Y.; Whitehead, G. F. S.; Young, R. J., Self-assembly of a layered two-dimensional molecularly woven fabric. *Nature* **588**, 429-435 (2020).
4. Ciengshin, T., Sha, R. & Seeman, N. C. Automatic molecular weaving prototyped by using single-stranded DNA. *Angew. Chem. Int. Ed.* **50**, 4419–4422 (2011).
5. Liu, Y.; Ma, Y.; Yang, J.; Diercks, C. S.; Tamura, N.; Jin, F.; Yaghi, O. M., Molecular Weaving of Covalent Organic Frameworks for Adaptive Guest Inclusion. *J. Am. Chem. Soc.* **140**, 16015-16019 (2018).
6. Zhao, Y.; Guo, L.; Gándara, F.; Ma, Y.; Liu, Z.; Zhu, C.; Lyu, H.; Trickett, C. A.; Kapustin, E. A.; Terasaki, O.; Yaghi, O. M., A Synthetic Route for Crystals of Woven Structures, Uniform Nanocrystals, and Thin Films of Imine Covalent Organic Frameworks. *J. Am. Chem. Soc.* **139**, 13166-13172 (2017).
7. Liu, Y., Diercks, C.S., Ma, Y., Lyu, H., Zhu, C., Alshimmri, S.A., Alshihri, S. and Yaghi, O.M., 3D covalent organic frameworks of interlocking 1D square ribbons. *J. Am. Chem. Soc.* **141**, 677-683 (2018).
8. Liu, Y.; Ma, Y.; Zhao, Y.; Sun, X.; Gándara, F.; Furukawa, H.; Liu, Z.; Zhu, H.; Zhu, C.; Suenaga, K.; Oleynikov, P.; Alshammari, A. S.; Zhang, X.; Terasaki, O.; Yaghi, O. M., Weaving of organic threads into a crystalline covalent organic framework. *Science* **351**, 365-369 (2016).

9. Kramer, R., Lehn, J.M. and Marquis-Rigault, A., Self-recognition in helicate self-assembly: spontaneous formation of helical metal complexes from mixtures of ligands and metal ions. *Proc. Natl. Acad. Sci.* **90**, 5394-5398 (1993).
10. Lehn, J. M., Toward complex matter: Supramolecular chemistry and self-organization. *Eur. Rev.* **99**, 4763-4768 (2002).
11. Piguet, C., Bernardinelli, G. and Hopfgartner, G., Helicates as versatile supramolecular complexes. *Chem. rev.* **97**, 2005-2062 (1997).
12. Ayme, J.-F.; Beves, J. E.; Campbell, C. J.; Leigh, D. A., Template synthesis of molecular knots. *Chem. Soc. Rev.* **42**, 1700-1712 (2013).
13. Dietrich-Buchecker, C.; Rapenne, G.; Sauvage, J.-P.; De Cian, A.; Fischer, J., A Dicopper(I) Trefoil Knot with m-Phenylene Bridges between the Ligand Subunits: Synthesis, Resolution, and Absolute Configuration. *Eur. J. Chem.* **5**, 1432-1439 (1999).
14. Dietrich-Buchecker, C.; Sauvage, J.-P., Lithium templated synthesis of catenanes: efficient synthesis of doubly interlocked [2]-catenanes. *Chem. Commun.* **7**, 615-616 (1999).
15. Gemmi, M. and Oleynikov, P., Scanning reciprocal space for solving unknown structures: Energy filtered diffraction tomography and rotation diffraction tomography methods. *Z. Kristallogr.*, **228**, 51–58 (2013).
16. Zhang, Y.-B., Su, J., Furukawa, H., Yun, Y., Gándara, F., Duong, A., Zou, X., and Yaghi, O. M., Single-crystal structure of a covalent organic framework. *J. Am. Chem. Soc.* **135**, 16336–16339 (2013).
17. Nannenga, B. L., MicroED methodology and development. *Struct. Dyn.* **7**, 014304 (2020).
18. Nannenga, B. L.; Gonen, T., The cryo-EM method microcrystal electron diffraction (MicroED). *Nat. Methods* **16**, 369-379 (2019).

19. Kabsch, W., XDS. *Acta Crystallogr. D*, **66**, 125-132 (2010).
20. Xu, H.-S.; Luo, Y.; Li, X.; See, P. Z.; Chen, Z.; Ma, T.; Liang, L.; Leng, K.; Abdelwahab, I.; Wang, L.; Li, R.; Shi, X.; Zhou, Y.; Lu, X. F.; Zhao, X.; Liu, C.; Sun, J.; Loh, K. P., Single crystal of a one-dimensional metallo-covalent organic framework. *Nat. Commun.* **11**, 1434 (2020).
21. Fang, Q., Sui, C., Wang, C., Zhai, T., Zhang, J., Liang, J., Guo, H., Sandoz-Rosado, E. and Lou, J., 2021. Strong and flaw-insensitive two-dimensional covalent organic frameworks. *Matter* **4**, 1017–1028 (2021).
22. Tan, J.C. and Cheetham, A.K., Mechanical properties of hybrid inorganic–organic framework materials: establishing fundamental structure–property relationships. *Chem. Soc. Rev.* **40**, 1059-1080 (2011).
23. Zeng, Y., Gordiichuk, P., Ichihara, T., Zhang, G., Sandoz-Rosado, E., Wetzel, E.D., Tresback, J., Yang, J., Kozawa, D., Yang, Z. and Kuehne, M., Irreversible synthesis of an ultrastrong two-dimensional polymeric material. *Nature* **602**, 91-95 (2022).

Acknowledgments:

This research was supported by King Abdulaziz City for Science and Technology (KACST) as part of a joint KACST–UC Berkeley Center of Excellence for Nanomaterials for Clean Energy Applications, and the Defense Advanced Research Projects Agency (DARPA) under contract HR001-119-S-0048. We acknowledge the College of Chemistry Nuclear Magnetic Resonance Facility for resource instruments at UC Berkeley, which are partially supported by NIH S10OD024998, and staff assistance from Dr. Hasan Celik. We would like to acknowledge the use of the Titan Krios at the Eyring Materials Center at Arizona

State University and the funding of this instrument by NSF MRI 1531991. Prof. Jorge A. R. Navarro is grateful to Spanish Ministry of Universities for a Salvador Madariaga-Fulbright grant (PRX21/00093). The authors thank Prof. George Lisensky (Beloit College) and Haoze Wang for helpful discussions. X. H. was partially supported by the Postdoctoral Innovative Support Program (BX20190195) and the China Postdoctoral Science Foundation (2019M661483).

Author contributions:

X.H., Y.C. and O.Y. conceived the idea and led the project. X.H., T.M. conducted the synthesis and crystal growth. B.N., Y.X. and Y.Z. carried out electron diffraction study and structure refinement. P.K., J.K. and R.R performed the AFM mechanical test. K.W. and Z.R contributed to material characterization; X.H. and O.Y. wrote the manuscript with help from S.E.N. and J.N. All authors discussed and revised the manuscript.

Competing interests:

The authors declare no competing interests.

Additional information

Supplementary Information

The online version contains supplementary material available at <https://doi.org/>

Data and materials availability

Experimental data and characterization data are provided in the Supplementary Information. Crystallographic data for the two crystals (tentatively assigned to right-handed) reported in this Article have been deposited at the Cambridge Crystallographic Data Centre, under deposition numbers CCDC 2237071 (COF-524-Cu), 2237072 (COF-525-Cu), 2237073 (Cu₃(PPPN)₂(BF₄)₃), 2238919

(Cu₂(PPN)₂(BF₄)₂). Copies of the data can be obtained free of charge via <https://www.ccdc.cam.ac.uk/structures/>.

Correspondence and requests for materials should be addressed to Yong Cui and Omar M. Yaghi.

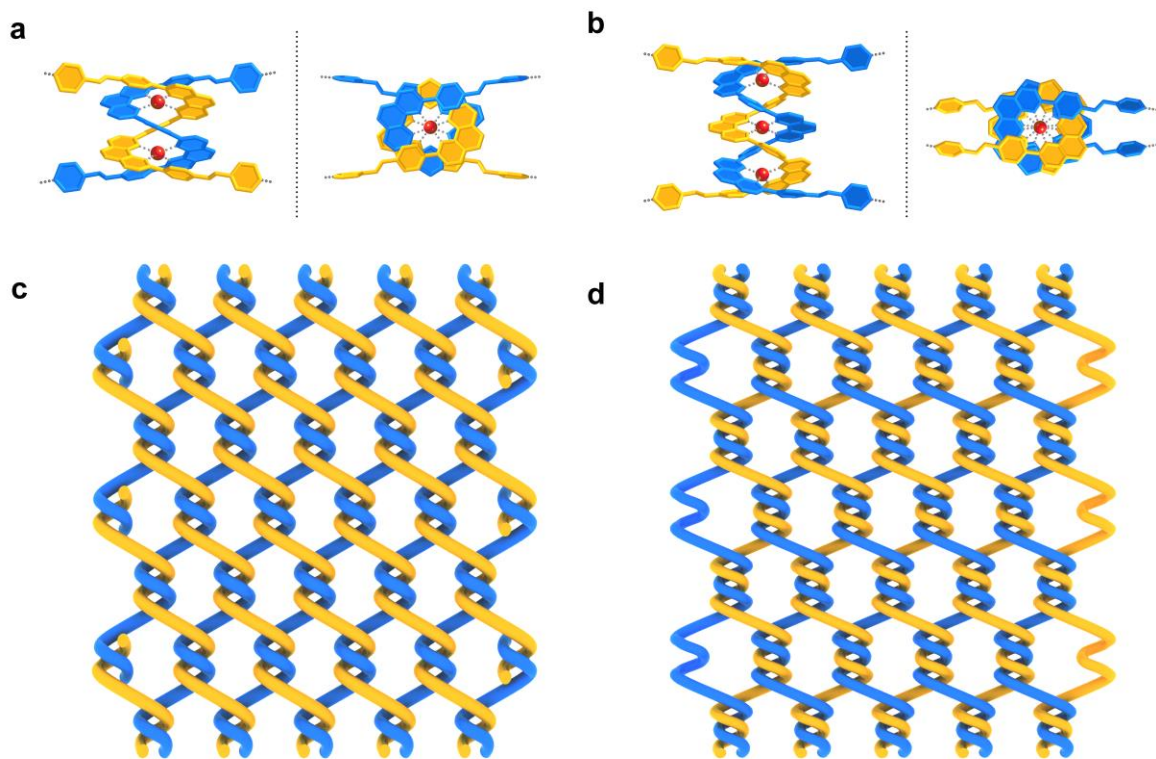


Fig. 1. Illustrations of woven threads in two dimensions. The complex (Left: side view; Right: top view) with two (a) and three (b) copper(I) ion centers generates helicates with planar geometry, which directs the formation of 2D woven frameworks (c, d).

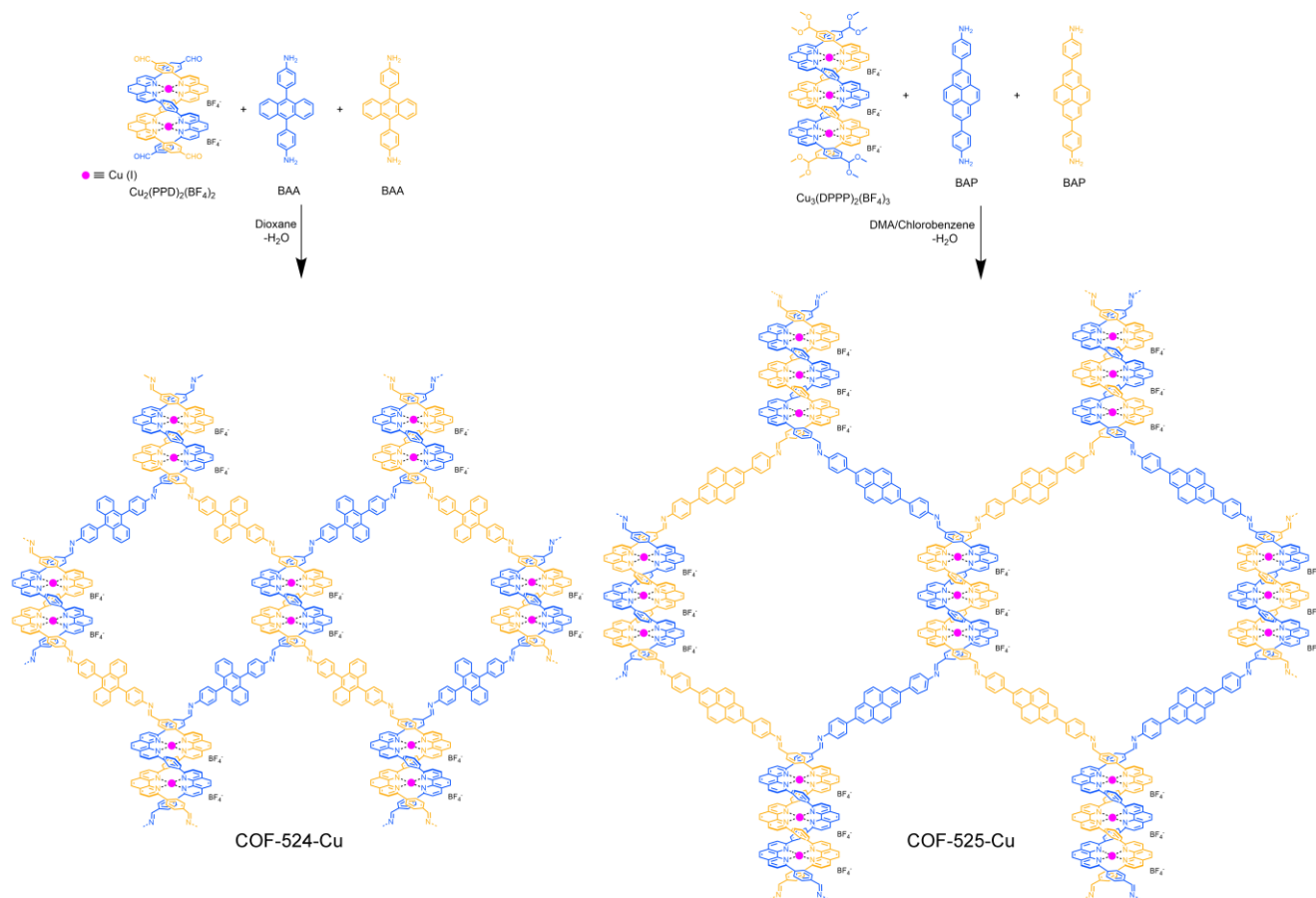


Fig. 2 | General strategy for the design and synthesis of woven frameworks resembling chicken wire structures. COF-524-Cu (left) and 525-Cu (right) constructed from organic threads using copper(I) as a template to make two-dimensional extended weaving structures.

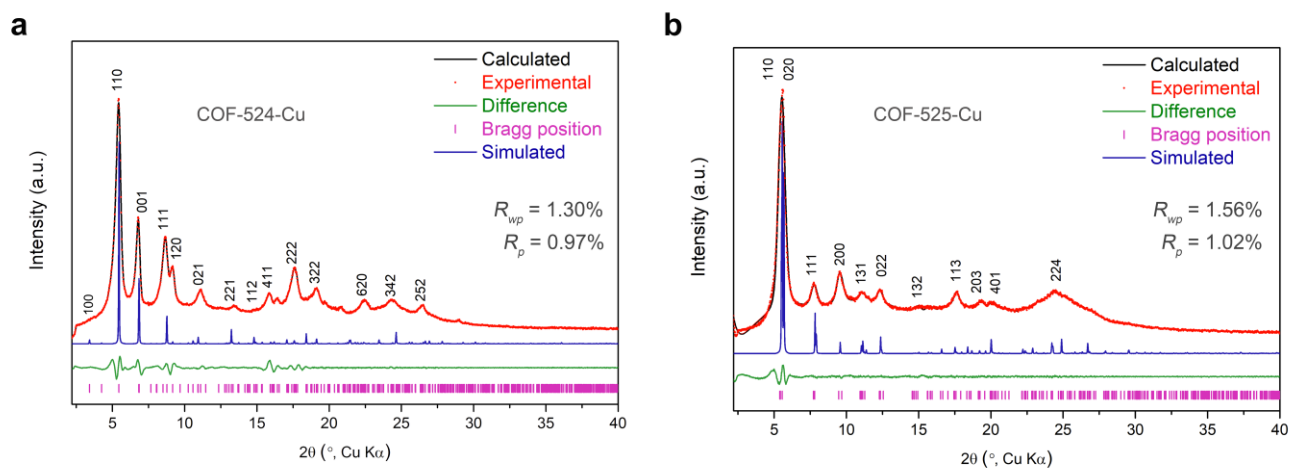


Fig. 3 | The PXRD refinement. Indexed PXRD pattern of the activated COF-524-Cu (a) and 525-Cu (b) samples (orange) and Pawley refinement (black) of the unit cell from the modeled structures.

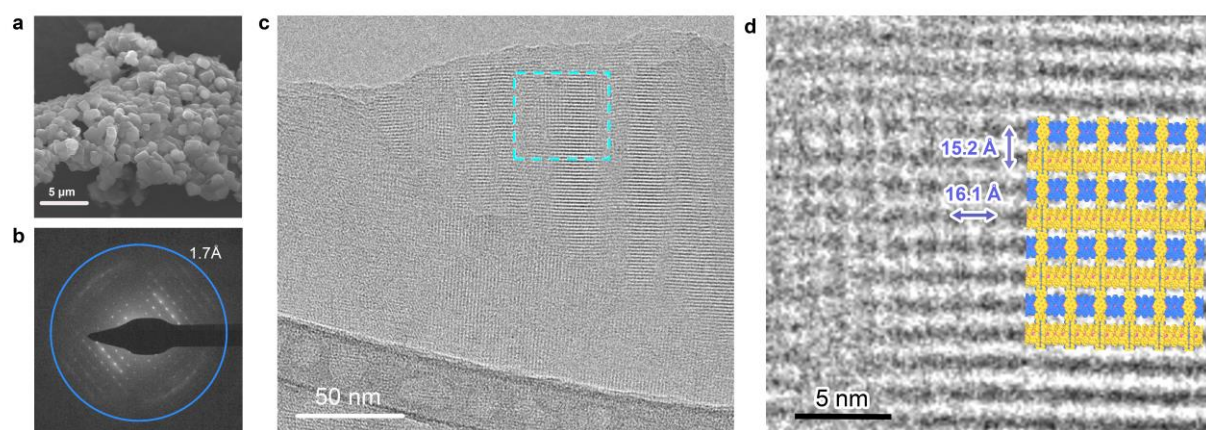


Fig. 4 | Electron microscopy studies of COF-525-Cu. (a) SEM micrographs of the COF-525-Cu crystallites indicate a single morphological phase with a homogeneous distribution of crystal sizes of ~ 100 nm. (b) Electron diffraction pattern acquired from a selected area of the crystal confirms the single crystalline nature of the particles. (c) HRTEM image of COF-525-Cu. (d) Magnified view of the highlighted area in panel d overlaid with a structure model showing good agreement along [100].

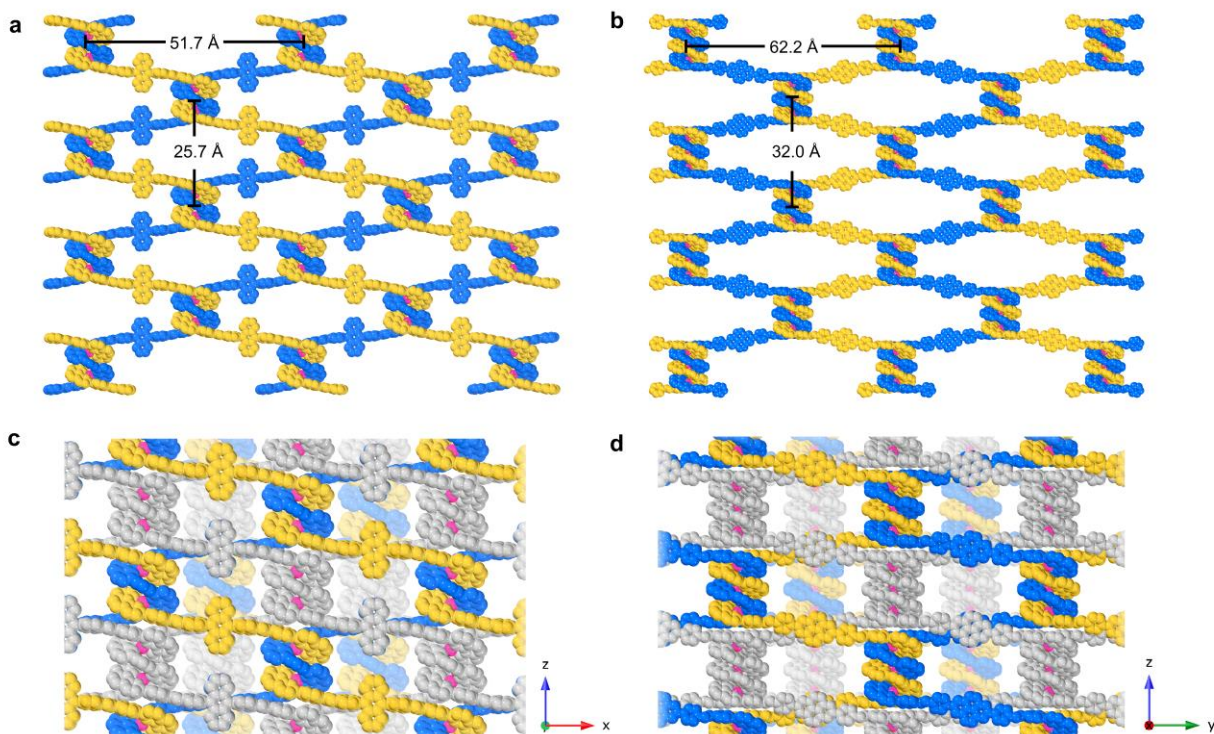


Fig. 5 | Modeled crystal structures of the woven COFs. **COF-524-Cu:** **a**, The diagonal blue and yellow linear threads are woven to form the 2D structure with $25.7 \times 51.7 \text{ \AA}$ meshes. Each of the threads is periodically crossing all threads that are orthogonal to it. **c**, Blue, yellow, and white threads are mutually woven into a two-fold interpenetrated pattern within one layer. Each layer is staggered along the a-axis. **COF-525-Cu:** **b**, The 2D structure formed by the weaving of adjacent parallel zigzag threads (blue and yellow) with $32.0 \times 62.2 \text{ \AA}$ meshes. Each of the threads is periodically crossing all threads that are parallel to it. **d**, Blue, yellow, and white threads are mutually woven into a two-fold interpenetrated pattern within one layer. Each layer is staggered along b-axis. All hydrogen atoms and BF_4^- ions are omitted for clarity. Copper atoms, pink.

